

## PDF hosted at the Radboud Repository of the Radboud University Nijmegen

The following full text is a preprint version which may differ from the publisher's version.

For additional information about this publication click this link.

<http://hdl.handle.net/2066/173503>

Please be advised that this information was generated on 2017-12-05 and may be subject to change.

## A SEARCH FOR MILLISECOND-PULSAR RADIO EMISSION FROM THE FAINT QUIESCENT SOFT X-RAY TRANSIENT 1H 1905+000

K. MIKHAILOV<sup>1,2</sup>, J. VAN LEEUWEN<sup>2,1</sup>, P. G. JONKER<sup>3,4</sup>

Draft version March 29, 2017

## ABSTRACT

Transitional millisecond pulsars (tMSPs) switch between an accretion-powered state *without* radio pulsations and a rotation-powered state *with* radio pulsations. In the former state, they are X-ray bright, in the latter X-ray dim. Soft X-ray transients (SXTs) undergo similar switches in X-ray, between “high” states with bright X-ray outbursts and a “low” state of quiescence. The upper limit on the quiescent X-ray luminosity of SXT 1H 1905+000 suggests that its luminosity might be similar to that of the known tMSPs. A detection of radio pulsations would link SXTs more strongly with tMSPs; and thus e.g. put stricter constraints on tMSP transitional timescales, through the connection with the well-known SXT periods of quiescence. A non-detection allows us, based on the telescope sensitivity, to estimate how likely these sources are to pulsate in radio. Over a ten-year span, 2006-2015, we carried out targeted radio observations at 400/800 MHz with Arecibo, and searched for radio pulsations from the quiescent SXT 1H 1905+000. None of the observations have revealed radio pulsations from the targeted SXT. For a 1-ms pulsar our flux density upper limit is  $10.3 \mu\text{Jy}$ . At an assumed distance of 10 kpc this translates to a pseudo-luminosity upper limit of  $1.0 \text{ mJy kpc}^2$ , which makes our search complete to  $\sim 85\%$  of the known MSP population. Given the high sensitivity, and the generally large beaming fraction of millisecond pulsars, we conclude that SXT 1H 1905+000 is unlikely to emit in radio as a transitional millisecond pulsar.

**Keywords:** stars: neutron – pulsars: general – stars: individual (1H 1905+000) – X-rays: binaries

## 1. INTRODUCTION

Recent multiwavelength observations have uncovered a new type of neutron star binaries, the transitional millisecond pulsars (tMSPs), that switch between two separate states. The first state, an accretion-powered or low mass X-ray binary (LMXB, Burderi & Di Salvo 2013) state, is usually described by an accretion disk, formed by matter transfer from a binary companion to a neutron star (NS). It features thermal X-ray emission thought to arise close to the NS surface. In this state, pulsar radio emission may be hampered by e.g. surface heat (this work) or by a disk passing through the pulsar’s light cylinder (Archibald et al. 2009). The flat-spectrum continuum radio emission can be caused by collimated polar outflows (Deller et al. 2015).

The second state, a rotation-powered or radio millisecond pulsar (MSP, Bhattacharya & van den Heuvel 1991) state, lacks the surrounding disk but instead is characterised by two oppositely directed coherent radio beams from the NS polar cap region. The inner part of the disk is blown away possibly by the “propeller” effect (Illarionov & Sunyaev 1975) or by  $\gamma$ -ray photons from the pulsar magnetosphere (Takata et al. 2014). Both the LMXB and MSP states are illustrated in Fig. 1.

Which physics underlies the tMSP switches between “pulsar-off” and “pulsar-on” states? And how do they evolve? Do all near-quiescent accreting millisecond X-ray pulsars with coherent pulsations of frequency range between 150-

600 Hz (AMXPs, Patruno & Watts 2012) end up as transitional radio pulsars? Transitions between two states might be explained via the interplay of the mass accretion rate and its corresponding ram pressure, and the radiation pressure exerted by the pulsar wind (Campana et al. 1998; Burgay et al. 2003; Archibald et al. 2009).

To date, three tMSPs are known to undergo transitions:

- (i) PSR J1023+0038 (Archibald et al. 2009) established the tMSP class. The neutron star rotates every 1.69 ms and 4.8 hr around its rotational axis and the centre of the binary mass, respectively, and has a  $\sim 0.2 M_{\odot}$  companion;
- (ii) PSR J1824-2452I is a binary source in the globular cluster M28 (and thus henceforth referred to as M28-I, Papitto et al. 2013), and spins every 3.93 ms. It also has a  $\sim 0.2 M_{\odot}$  companion, but its orbital period is about 11 hr. This is so far the only tMSP that also shows outbursts / Type I X-ray bursts similar to soft X-ray transients;
- (iii) PSR J1227-4853 (de Martino et al. 2010; Bassa et al. 2014; Roy et al. 2015), also spins with a 1.69 ms period. It takes 6.7 hr for the source to orbit the center of mass. The companion has a mass between  $0.17 M_{\odot}$  and  $0.46 M_{\odot}$ .

MSPs with companions of similar mass are known as “redbacks” (Roberts 2013). The MSP-state X-ray luminosity of all three tMSPs is also of the same order:  $L_X \sim 10^{30}-10^{32} \text{ erg s}^{-1}$  (Linares et al. 2014). One tMSP (M28-I) was found in an X-ray bright outburst state with  $L_X \sim 10^{34}-10^{37} \text{ erg s}^{-1}$ , but similar to the two other tMSPs (PSR J1023+0038 and PSR J1227-4853) it also exhibits a disk-state at lower luminosity  $L_X \sim 10^{32}-10^{34} \text{ erg s}^{-1}$ . The latter two also provide  $\gamma$ -ray emission (Stappers et al. 2014; Johnson

<sup>1</sup> Anton Pannekoek Institute for Astronomy, University of Amsterdam, Science Park 904, PO Box 94249, 1090 GE Amsterdam, The Netherlands; K.Mikhailov@uva.nl

<sup>2</sup> ASTRON, the Netherlands Institute for Radio Astronomy, PO Box 2, 7990 AA, Dwingeloo, The Netherlands

<sup>3</sup> SRON, the Netherlands Institute for Space Research, Sorbonnelaan 2, 3584 CA, Utrecht, the Netherlands

<sup>4</sup> Department of Astrophysics/IMAPP, Radboud University, P.O. Box 9010, 6500 GL Nijmegen, The Netherlands

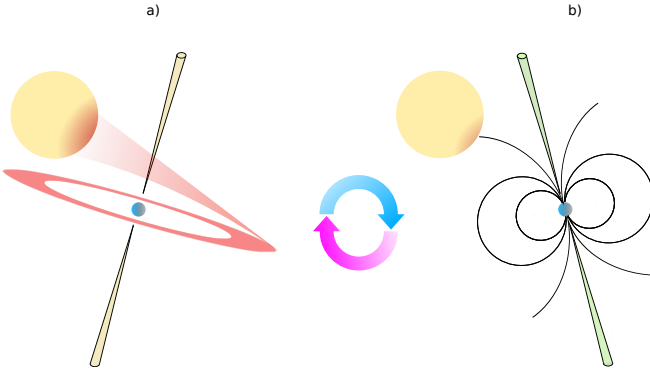


**Figure 1.** Two states of transitional binaries: a) an accretion-powered state with jets, collimated relativistic outflows (shown in yellow); b) a radio MSP state with a beamed radio emission (shown in green). Note that the radio pulsar beam is not necessarily in the same direction as the outflow. The red region on the companion signifies a) channelised or b) potentially on-going (but much weaker, see Sect. 5.3) accretion.

et al. 2015) which establishes a putative link with a few variable  $\gamma$ -ray LMXBs (Strader et al. 2015; Bogdanov & Halpern 2015). Based on multiwavelength tracking of these sources, the estimated timescale between disk-MSP transitions is of order a decade (Tam et al. 2014; Johnson et al. 2015). At the same time, transitional timescales for tMSPs were constrained to be much shorter – from a few days to a few months (Stappers et al. 2013; Papitto et al. 2013; Bassa et al. 2014).

The hypothesis we aim to test in this paper is whether tMSPs are related to the NS soft X-ray transients (SXTs, Stella et al. 1994). SXTs undergo transitions between two X-ray states: a bright “outburst” state ( $L_X \sim 10^{35} - 10^{38} \text{ erg s}^{-1}$ ), sometimes with regular bright thermonuclear flashes of type I X-ray bursts from the NS surface (Galloway et al. 2008), and a much fainter “quiescent” state ( $L_X \sim 10^{30} - 10^{33} \text{ erg s}^{-1}$ ) where the source remains dim (see, e.g. Campana et al. 1998; Yakovlev & Pethick 2004, for a review). Besides, SXTs outburst rise/decay times are also within days – months range (Campana et al. 1998). Finally, the  $B > 10^8 \text{ G}$  magnetic fields constrained for some X-ray transients (e.g., Di Salvo & Burderi 2003) are of the same order as for AMSPs/tMSPs (see, e.g., Table 4 from Patruno & Watts 2012). The similarities with the X-ray luminosity, magnetic field, and transitional timescales of the tMSP makes us wonder if in this quiescent state the radio pulsar might appear.

It is not yet clear which conditions a binary system should possess in order to undergo state switches; SAX J1808.4-3658 (Wijnands & van der Klis 1998; Chakrabarty & Morgan 1998; Hartman et al. 2008) is a good representation of an AMXP with about a 2.5 ms period and a typical  $10^8 - 10^9 \text{ G}$  magnetic field that also experiences outbursts of  $10^{36} \text{ erg s}^{-1}$  X-ray luminosity (see, e.g., Hartman et al. 2009) but so far has not been seen in radio (Burgay et al. 2003; Iacolina et al. 2010; Patruno et al. 2016). Given that lack of understanding on transitional-pulsar system parameters, we seek to expand the population by investigating tMSP candidates, and potentially link SXTs and tMSPs.

One of the best such candidate systems is SXT 1H 1905+000 (Jonker et al. 2006, 2007). It is a very low luminosity NS binary, involving a white or a brown dwarf companion ( $M_{\text{comp}} \approx 0.01 - 0.05 M_{\odot}$ ) and an extremely short orbit (the orbital period  $P_{\text{orb}} \lesssim 1.33 \text{ hr}$ ). After about an 11-yr ( $L_X \approx 4 \times 10^{36} \text{ erg s}^{-1}$ ) outburst with several Type I X-ray bursts ending more than eighteen years ago, the source has remained quiescent.

The quiescent luminosity of SXT 1H 1905+000  $L_X \lesssim 1.8 \times 10^{30} \text{ erg s}^{-1}$  is the lowest among all known NS X-ray transients, which makes the source most closely related to the MSP class. As for hotter neutron stars, the radio pulsar emission may be inhibited via electron braking by inverse Compton scattering (see Sect. 5.2 and the references therein), the low effective temperature  $T_{\text{eff}} \lesssim 3.5 \times 10^5 \text{ K}$  of SXT 1H 1905+000 should allow particle to flow more freely (see, e.g., Supper & Trümper 2000). Therefore, the presumed MSP should be able to emit in radio. Past 25 ks (Jonker et al. 2006) and 300 ks (Jonker et al. 2007) Chandra X-ray observations did not detect the NS in quiescence. No new X-ray outbursts were detected in X-ray all-sky monitors, and the source stayed quiescent over the period covered in this paper. This also suggests that SXT 1H 1905+000 might be capable of producing pulsar radio emission.

Revealing radio pulsations in a quiescent SXT would link the timescales on which tMSPs switch, to known periods of SXT quiescence. That would be a first step to better understand the interaction between accretion, thermal and radio pulsar emission. In the remainder of this paper, Section 2 describes our observations of SXT 1H 1905+000. The data analysis for each targeted search is detailed in Sect. 3. Section 4 outlines the obtained results, followed by the discussion in Sect. 5, and conclusions in Sect. 6.

## 2. OBSERVATIONS

We have conducted three targeted observations of the SXT 1H 1905+000 spanning a period of almost ten years. All three observations were performed with the 305-m William E. Gordon radio telescope at Arecibo<sup>1</sup>, using the L-wide (first two observations) and S-low (third observation) receivers<sup>2</sup>. The setup specifications, detailed in Table 1, are summarized below.

The first targeted search consisted of two separate observing sessions on 2006 May 20 and June 25. We used the Wide-band Arecibo Pulsar Processor (WAPP<sup>3</sup>, Dowd et al. 2000) so that each 128  $\mu\text{s}$  it separately recorded four sets of 512 spectral frequency channels, each 0.195 MHz wide, of 16-bit total intensity. To avoid a frequency range often affected by radio-frequency interference (RFI) we split the recording over 100 and 300 MHz bands around 1120 and 1410 MHz, respectively.

For our second observation on 2015 April 14 we used the Puertorican Ultimate Pulsar Processing Instrument (PUPPI) backend<sup>4</sup>, with 800 MHz bandwidth and 2048 frequency channels. This resulted in the 1380 MHz central frequency, 0.390 MHz bandwidth per channel and the minimum sampling time of 41  $\mu\text{s}$ . All frequencies outside the L-wide receiver range of 1.15-1.73 MHz were zapped during the RFI masking stage in our search pipeline.

Finally, we carried out a third observation on 2015 August 26, with the same specifications as the second but at a higher central frequency  $\nu_{\text{obs}} = 2800 \text{ MHz}$ . That reduced potential scattering on the pulsar, and was less affected by RFI.

We first pointed Arecibo on a number of known pulsars to test both telescope and backend efficiencies. Test pulsars are given in Table 2 along with respective timespans, pulse periods, dispersion measures (DMs), duty cycles, nominal flux densities, and peak signal-to-noise ratios (S/Ns). These

<sup>1</sup> [http://www.naic.edu/index\\_scientific.php](http://www.naic.edu/index_scientific.php)

<sup>2</sup> <http://www.naic.edu/~astro/RXstatus/>

<sup>3</sup> <http://www.naic.edu/~wapp/>

<sup>4</sup> <http://www.naic.edu/~astro/guide/node11.html>

**Table 1**  
Observational setup for three different Arecibo observations of SXT 1H 1905+000.

Parameter	Value		
Project ID	p2204	p2994	p3013
Receiver (year)	L-wide (2006)	L-wide (2015)	S-low (2015)
Gain (K/Jy)	10	10	8
System Temp (K)	30	30	35
Native Polarization	d u a l   l i n e a r		
Sample time ( $\mu$ s)	128	40.96	40.96
Integration time (s)	3600	3600	2150
Bandwidth (MHz)	300	500	500
Central freq (MHz)	1410	1380	2800
Channels	1536	2048	2048
Subbands	64	64	64

**Note.** — For the first 2006 observation we list only the dataset with the larger contiguous band.

**Table 2**  
Parameters for test observations of two known pulsars.

Pulsar	$t_{\text{int}}$ (s)	$P$ (ms)	DM (pc cm $^{-3}$ )	$W_{50}/P$	$S_{\nu}$ (mJy)	$S/N_{\text{peak}}$
PSR J1857+0943	300	5.362	13.3	$9.7 \times 10^{-2}$	5.0	39.20 <sup>a</sup>
					1.4	327.35 <sup>c</sup>
	600 (900) <sup>a</sup>					590.64 <sup>a</sup>
PSR J1906+0746	275 <sup>b</sup>	144.073	217.20	$4.2 \times 10^{-3}$	0.55	18.10 <sup>b</sup>
	900 <sup>c</sup>				0.16	(...) <sup>c</sup>

<sup>a</sup> 2006 L-wide observation

<sup>b</sup> 2015 L-wide observation

<sup>c</sup> 2015 S-low observation

**Note.** — In 2006, PSR J1857+0943 was observed in session 1, and PSR J1906+0746 in both sessions, but with different integration times.  $W_{50}/P$  is the pulse duty cycle ( $W_{50}$  is the pulse width at half-peak height),  $S_{\nu}$  is the pulsar flux density based on ATNF pulsar catalogue, and  $S/N_{\text{peak}}$  is the integrated signal-to-noise ratio at the correct DM.

were generally detected as predicted. The absence of PSR J1906+0746 at 2.8 GHz was not unexpected as geodetic precession causes its radio beam to ever more miss Earth (van Leeuwen et al. 2015).

We pointed the telescope at the best known position at the time, RA=19<sup>h</sup>08<sup>m</sup>27<sup>s</sup>, DEC=+00°10′08″ (J2000). This puts the Arecibo beam well over the improved position published later in Jonker et al. (2006), as discussed in Sect. 5.1. We observed for 3400 s and 3600 s during two first search sessions, for 3600 s during the second search session, and for about 2150 s during the third search session.

### 3. ANALYSIS

All our observations were analysed on the Dutch national supercomputer, Cartesius<sup>5</sup>. For the search itself we adopted the PRESTO pulsar search toolkit<sup>6</sup> (Ransom 2001).

#### 3.1. 2006 L-wide observation

The WAPP backend produces multiple sequential time series, divided into 100 MHz bandwidth slices<sup>3</sup>. We used the dataset with the contiguous 300 MHz bandwidth for the direct search, and the 100-MHz dataset only for verification. The estimated distance to the source is 7-10 kpc (Jonker & Nelemans 2004), and according to the galactic electron density model (ne2001<sup>7</sup>, Cordes & Lazio 2002) the free electron content amounts 250-350 pc cm $^{-3}$ , respectively. As the

ne2001 model continues to get supplemented and improved, especially for sources located far along the Galactic plane where most of cold interstellar plasma resides (see, e.g., Yusefov & Küçük 2004; Cordes 2004; Sun & Reich 2010), we searched out to a  $3 \times$  larger maximum DM, over a range from 0 to 1000 pc cm $^{-3}$ . For the 80 min orbital period and an ultra-compact binary ( $M_{\text{comp}} \simeq 0.05 M_{\odot}$ ) one should expect a high orbital acceleration (Johnston & Kulkarni 1991). Using a 0.05 ms sampling time, we employed the maximum possible number of acceleration drift (Fourier) bins allowed in PRESTO ( $z_{\text{max}} = 0, 5, 100, 200, 1200$ ).

Assuming a circular, edge-on orbit ( $e = 0$ ,  $\theta = 90^\circ$ ), the estimated orbital acceleration is  $a = (2\pi)^{4/3} \times G^{1/3} \times M_{\text{comp}} \times \sin \theta / (P_{\text{orb}}^{4/3} \times (M_{\text{ns}} + M_{\text{comp}})^{2/3}) \simeq 28.6 \text{ m s}^{-2}$ , at the upper boundary of the limiting range of linear orbital accelerations  $a^* \approx 30 \text{ m s}^{-2}$  of most known pulsar binaries (Camilo et al. 2000). As the pulsar acceleration completely reverses every half of the orbit, it is reasonable to have an integration time within a small fraction of the orbital period (generally,  $0.1 P_{\text{orb}}$ , Ransom et al. 2003; Burgay et al. 2003). For this reason, we also split up the time series to  $t_{\text{int}} \simeq 410 \text{ s}$  ( $\simeq 7 \text{ min}$ ) and performed the search on these shorter sets, each with less Doppler smearing. Knowing our observing duration, and aiming to be sensitive down to a period  $P = 1 \text{ ms}$ , we would need  $N_{\text{drift}} = a \times t_{\text{int}}^2 / (c \times P) \simeq 20$  Fourier bins. This is well in line with our covered bin range, even for a more massive companion or a faster MSP.

The searches over the 7-min sets have an additional sensitivity benefit if this pulsar, like other low-mass binaries, is eclipsed over part of the binary orbit (Luo & Melrose 1995, also see Sect. 5.4). Shorter integrations then suffer less from the addition of noise, without periodic signal, during the eclipse.

After a number of standard periodic search steps (RFI masking, dedispersion, FFT transform, red-noise removal, RFI birdies zapping, and accelerated search; also see Mikhailov & van Leeuwen 2016), all potential candidates were ranked and inspected according to their characteristic plots (pulse and frequency channels profiles, DM curve, and  $P - \dot{P}$  map, see, e.g., Fig. 2).

#### 3.2. 2015 L-wide observation

In the 2015 1.4-GHz observations using PUPPI, the full bandwidth was recorded, including bands prone to RFI. Those were excised in the pipeline, strongly reducing the effective band width as expected. We again carried out an acceleration search but now up to 100 Fourier bins (5 times an estimated value, see above). We did employ time-series slicing, and other search pipeline steps were also kept the same as in the 2006 observation.

#### 3.3. 2015 S-low observation

In order to avoid the RFI-contaminated part of the spectrum present in the 1.4 GHz data, and to reduce the potential interstellar scattering smearing present there, we also performed a 2.8-GHz (S-low band) observation, with otherwise identical settings as the 1.4 GHz setup.

#### 3.4. Single-pulse search

Some pulsars do not emit periodically, but only sporadically – such sources are referred to as rotating radio transients (RRATs, McLaughlin et al. 2006). For such pulsars, data folding mostly adds noise, and therefore single-pulse investigations are more effective. As millisecond pulsars emit

<sup>5</sup> <https://surfsara.nl/systems/cartesius>

<sup>6</sup> <https://github.com/scottansom/presto>

<sup>7</sup> <http://www.nrl.navy.mil/rsd/RORF/ne2001/>



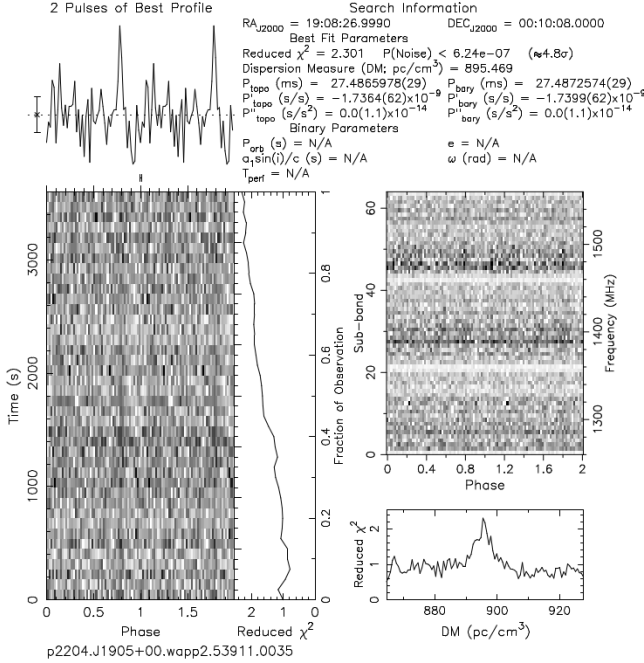


**Figure 2.** Representation of one of the most promising pulse configurations during the 2006 observation. Unfortunately, the candidate was only present in the second session. Moreover, further search identified that there were more similar instances for multiple DM values – a property inherent to RFI sources.

around 10 – 1000 pulses per second, it is hard to resolve individual pulses since their S/N is normally quite low.

At the same time, some pulsars occasionally emit giant pulses – a type of non-frequent short duration radio pulses that can greatly exceed (by 2 – 3 orders of magnitude) the mean flux density of normal pulses from those pulsars. Around ten millisecond pulsars are now known to emit giant pulses (Knight 2006; Bilous et al. 2015), the most pronounced examples being PSR B0531+21 (the Crab), PSR B0833-45 (Vela), and PSR B1937+21.

The most common S/N values found for candidates in our search were from 5 to 7, below our single-pulse detection threshold  $S/N_{\min} \geq 8$ . Single-pulse thresholds can in practice be set somewhat lower than periodicity thresholds (cf. Eq. 1) without producing overwhelming numbers of candidates. None of the candidates above this threshold were identified as genuine pulses. Most showed a monotonic profile of S/N distribution along adjacent DM values, behaviour typical for RFI.

#### 4. RESULTS

Neither the 2006 nor the 2015 observations reveal any good candidates for the potential radio MSP counterpart towards 1H 1905+000.

The RFI situation at 1.4 GHz likely impeded the identification of genuine radio pulses from 1H 1905+000; especially the 2015 observation, where the bandwidth increase over 2006 mostly added bands of unprotected, multi-use spectrum, contained significant amounts of RFI that resulted in the elimination of some frequency coverage, thus diminishing the potential candidate S/N compared to an RFI-free ideal.

Using the radiometer equation (Bhattacharya 1998), we can

**Table 3**

Estimated instrumental ( $W_{\text{smear}}$ ) and scattering ( $W_{\text{scatter}}$ ) broadening, minimum flux density  $S_{\min}$ , pseudo luminosity  $L_{\text{pseudo}}$  as well as search completeness  $C_{\text{search}}$  for 1H 1905+000 at a distance of  $d = 7$  kpc ( $DM = 250 \text{ pc cm}^{-3}$ ) and  $d = 10$  kpc ( $DM = 350 \text{ pc cm}^{-3}$ ).

$d$ (kpc)	$W_{\text{smear}}$ (ms)	$W_{\text{scatter}}$ (ms)	$S_{\min}$ ( $\mu\text{Jy}$ )	$L_{\text{pseudo}}$ (mJy kpc <sup>2</sup> )	$C_{\text{search}}$ (%)
2006 L-wide observation					
7	0.23	$8.4 \times 10^{-3}$	11.8	0.6	89.72
10	0.27	0.01	13.0	1.3	76.64
2015 L-wide observation					
7	0.20	$8.5 \times 10^{-3}$	8.5	0.4	91.59
10	0.28	0.01	10.3	1.0	84.11
2015 S-low observation					
7	0.06	$0.4 \times 10^{-3}$	10.8	0.5	55.14
10	0.07	$0.6 \times 10^{-3}$	11.1	1.1	31.78

**Note.** — All estimates are tabulated for the lowest expected integer spin period  $P_{\min} = 1$  ms.

set an upper limit on the source flux density:

$$S_{\min} = \beta \frac{(S/N_{\min}) T_{\text{sys}}}{G \sqrt{n_p} \Delta \nu t_{\text{int}}} \sqrt{\frac{W}{P - W}}. \quad (1)$$

Here,  $\beta$  is a digitisation factor and is normally around 1,  $S/N_{\min}$  is the minimum distinguishable S/N from a potential pulsar,  $T_{\text{sys}} = T_{\text{sys,receiver}} + T_{\text{sky}}$  is the overall system temperature. The L-wide and S-low receiver temperatures are  $T_{\text{sys,LW}} \sim 25$  K and  $T_{\text{sys,SL}} \sim 35$  K, respectively. The sky temperature  $T_{\text{sky}}$  was interpreted from 408 MHz contour maps (Haslam et al. 1982) and scaled to 1400 and 2800 MHz using the Lawson et al. (1987) relation  $T_{\text{sky}} \propto \nu^{-2.6}$ , resulting in 5 and 0.8 K, respectively. Next,  $G_{\text{L-wide}} = 10 \text{ K/Jy}$  ( $G_{\text{S-low}} = 8 \text{ K/Jy}$ ) is the telescope gain<sup>8</sup>,  $n_p = 2$  for two polarisations,  $\Delta \nu$  is the frequency bandwidth, and  $t_{\text{int}}$  is the integration time.  $P$  and  $W$  are pulsar spin period and its pulse width, respectively. For typical MSP properties<sup>9</sup> (spin periods  $P \lesssim 20$  ms, and magnetic field strengths  $B \lesssim 10^9$  G), we find<sup>10</sup> the average pulse duty cycle  $\langle W_{50}/P \rangle$  to be  $0.10 \pm 0.07$ . We also include smearing effects into the pulse width broadening and bound it with a pulse period:  $W = W(P) = \sqrt{\langle W_{50}/P \rangle^2 \cdot P^2 + W_{\text{smear}}^2 + W_{\text{scatter}}^2}$ , where  $W_{\text{smear}}$  is the instrumental (channel, subband, DM<sub>step</sub>, sampling) smearing, and  $W_{\text{scatter}}$  is the scattering broadening along the line of sight. For the  $S/N_{\min}$  we follow the usual<sup>11</sup> value of 10.

In Table 3 we list our set of flux-density upper limits. For the first 1.4 GHz we list only the result with the longer integration time  $t_{\text{int}} = 3600$  s. The limits from the 2015 1.4 GHz and 2.8 GHz observations are based on 500 MHz of usable bandwidth out of the 800 MHz total. We see that scattering is not expected to play a significant role in the sensitivity compared to other smearing effects and that it does not change much with increasing distance. We also derive the pseudo luminosity  $L_{\text{pseudo}} = S_{\min} d^2$ ; and the search completeness  $C_{\text{search}}$ , the

<sup>8</sup> <http://www.naic.edu/~astro/RXstatus/>

<sup>9</sup> [http://www.cv.nrao.edu/~sransom/Exascale\\_Radio\\_Searches\\_2014.pdf](http://www.cv.nrao.edu/~sransom/Exascale_Radio_Searches_2014.pdf)

<sup>10</sup> <http://www.atnf.csiro.au/research/pulsar/psrcat/> (catalogue version 1.54, Manchester et al. 2005)

<sup>11</sup> [http://www.astro.cornell.edu/~cordes/PALFA/palfa\\_snr\\_calcs.pdf](http://www.astro.cornell.edu/~cordes/PALFA/palfa_snr_calcs.pdf)

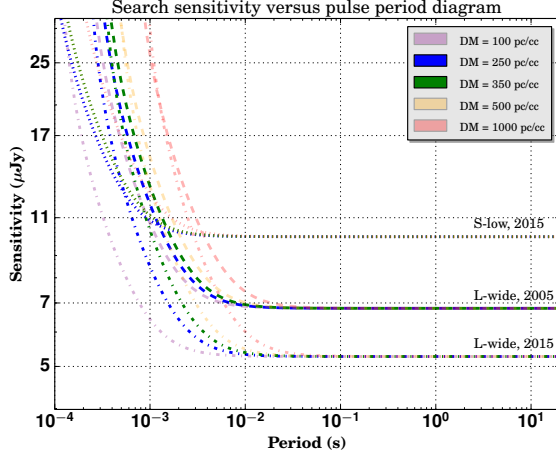


**Figure 3.** Sensitivity curves for each of the three 1H 1905+000 Arecibo observations for source DM = 100, 250, 350, 500, and 1000 pc cm<sup>-3</sup>. Smearing effects (both instrumental and astrophysical) are included. Highlighted are the expected dispersion measure lines for  $d = 7$  kpc (DM = 250 pc cm<sup>-3</sup>, shown in blue) and for  $d = 10$  kpc (DM = 350 pc cm<sup>-3</sup>, shown in green).

fraction of currently known pulsars that our search could have detected at the distance of 1H 1905+000 (Coenen et al. 2011).

The sensitivity of our searches is plotted in Fig. 3, for various possible pulse periods and dispersion measures. In what we think is the most realistic case, a DM = 250–350 pc cm<sup>-3</sup> (highlighted in the plot) at a pulse period of 10 ms, our deepest search, the 2015 L-wide observation, had a minimum detectable flux of about 5.5 μJy.

The resulting search efficiency, the fraction of known pulsars whose 1.4 GHz pseudo luminosity our survey could have detected at the distance of 1H 1905+000 is shown in Fig. 4. There we mark each Arecibo observation and estimated distance. To compare our 2.8 GHz S-low observation with the 1.4 GHz catalogue flux densities, we scaled down the search minimum detectable flux using a spectral index  $\alpha = -1.8$  (Maron et al. 2000). For each observation, we considered a pulse period range to be from 0.5 ms to 1 s, and the resulting spread for each observation is included in the Figure.

Our deepest search, the 2015 L-wide observation, was sensitive enough to find up to 92% of all catalogued pulsars (including the three known tMSPs) when put at 7 kpc.

Given the possibility that tMSPs shine only intermittently, the depth at the other observation epoch is equally important. In 2005 we too would have found around 75–90% of catalogued pulsars, and two out of three known tMSPs.

To validate our estimated completeness, we also searched a longer, 2015, 1.4 GHz dataset on PSR J1906+0746 that one of us took for long-term beam evolution studies (Desvignes et al., *in prep.*). At flux density  $S = 2 \pm 1 \mu\text{Jy}$  J1906+0746 is likely to be very close to our minimum detectable flux. We used the same setup as the other 2015 observations described in the current paper. We expected, from Eq. (1), a S/N of about 20, given the  $\sim 1$  hr integration time, duty cycle  $w_p = W_{50}/P$ , scattering contribution  $W_{\text{scatter}} < 0.01$  ms, and dispersion smearing contributions  $W_{\text{smear}} \approx 0.2 \text{ ms} \approx 0.05 w_p$ . The final pulse signal to noise obtained, for the best-fit acceleration, was 23.7, well in line with the expectation. This confirms our completeness limits are realistic.

## 5. DISCUSSION

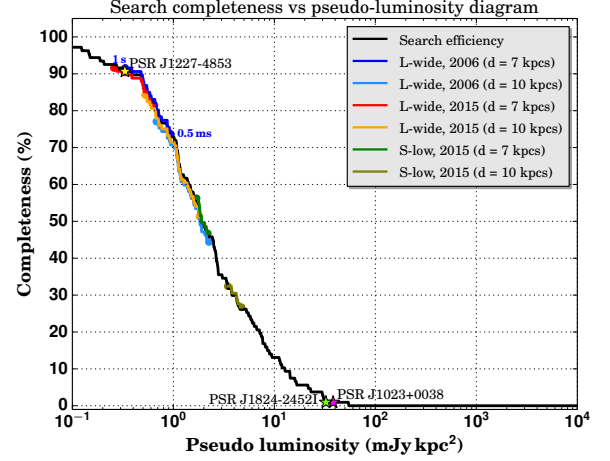


**Figure 4.** Search completeness compared to the ATNF-catalogue pseudo luminosities. Shown (slightly offset vertically for visibility) are the limits set by our observations. The range of values spanned by each observation is determined by the estimated pulse period, from 0.5 ms to 1 s (labeled as such for one example observation). The 2.8 GHz flux densities were scaled to 1.4 GHz for this plot. Stars represent pseudo luminosities of known tMSPs: J1023+0038 (magenta, Archibald et al. 2009), J1824-24521 (green, Papitto et al. 2013), J1227-4853 (yellow, Roy et al. 2015).

Given our high search completeness of  $\sim 90\%$  we are confident the source is currently not a radio MSP that shines our way. The putative pulsar itself can, of course, in principle be inclined away from Earth. However, we know that the opening angle of the MSP beams is usually quite broad, with beaming fractions of almost 100% in several beaming models (see, e.g., Lorimer 2008). We thus conclude that the source itself is not emitting radio pulses with luminosity above our limit.

So why is 1H 1905+000 not shining? Below we discuss how this could be related to e.g. surface heat, and past or current mass transfer.

### 5.1. Position, proper motion and the small Arecibo beam

The location of 1H 1905+000 is well known. Its outburst position error box,  $\alpha_{J2000.0} = 19^{\text{h}}08^{\text{m}}27^{\text{s}}.200 \pm 0^{\circ}.084$ ,  $\delta_{J2000.0} = +00^{\circ}10'09''10 \pm 0^{\circ}.087$  (Jonker et al. 2006), falls well within the Arecibo FWHM beam size at both L-wide ( $3.5' \times 3.1'$ ) and S-low ( $2.0' \times 1.8'$ ) receivers.

Could 1H 1905+000 have moved out of the Arecibo beam since that outburst position was derived? Even for the smallest, S-low 2.8 GHz beam, 1H 1905+000 should then travel with proper motion  $\mu = 5.4 \times 10^3 \text{ mas yr}^{-1}$ . For the largest distance of  $d = 10$  kpc, the characteristic system velocity  $v_{\text{NS}}$  needs to be  $4.74 \times \mu \times d \approx 2.6 \times 10^5 \text{ km s}^{-1}$  for the source to have moved outside the Arecibo beam which is an order of magnitude larger than seen so far for NS X-ray binaries.

### 5.2. Temperature and cooling emission

In the old normal MSPs we observe, the neutron star has cooled long ago and the thermal emission is nearly absent. In transitional MSPs, some thermal emission is only seen in the accreting phase. Yet SXTs are known to be strong thermal emitters even in quiescence, due to the reheating of the neutron star by nuclear reactions deep in the crust (Brown et al. 1998). Models for such heating (e.g. Haensel & Zdunik 2003; Yakovlev et al. 2006) can explain quiescent luminosities  $L_X \sim 10^{33} \text{ erg s}^{-1}$ , as observed. While the limit on 1H 1905+000 is much lower, as mentioned, its long and active state of accretion could still have left it hotter than the tMSPs,

which hardly appear to efficiently accrete (“radiatively inefficient” accretion, Archibald et al. 2015; Papitto et al. 2015; Deller et al. 2015) or spin up (Jaodand et al. 2016).

We here hypothesize that through this enhanced thermal emission over the tMSPs, 1H 1905+000 is prevented from generating radio emission. The increased intensity of soft X-ray photons could potentially be the extinguishing agent. While some such soft thermal photons coming from the hot NS surface are needed in certain models (e.g. Zhang et al. 1997) as the seed photons that inverse Compton scatter off the primary electrons, to form pair-producing photons; these same photons, once present in larger numbers, act as radiative brakes on these essential relativistic electrons (Kardashēv et al. 1984). The drag on these relativistic particles in the soft photon field in 1H 1905+000 and its hotter brethren may thus possibly quench the runaway cascade needed for robust radio emission.

If this is indeed the reason for the absence of radio emission from 1H 1905+000, such braking must already be significant at the temperature inferred by Jonker et al. (2007) of  $T_{\text{eff}} \lesssim 3.5 \times 10^5$  K, or  $kT \lesssim 30$  eV. Supper & Trümper (2000) modeled this dependence of inverse Compton scattering on temperature, for values of 100, 300, and 1000 eV. At 100 eV, the electrons suffer no weakening but achieve acceleration up to the maximum Lorentz factor  $\gamma \simeq 10^6$ . For mildly higher temperatures of 300 and 1000 eV, respectively, electrons are quickly braked and reach Lorentz factors of  $10^4$  and  $10^2$  only (Eq. 26 and Figs. 4–6 in Supper & Trümper 2000), likely hampering subsequent formation of radio emission. Thus, while this model does show there is a clear dependence of inverse Compton scattering on temperature, it cannot currently explain the case of 1H 1905+000.

To summarize: it seems likely that one of the main observational differences between SXTs and tMSPs, the higher temperatures of the former, is the cause of the lack of radio emission on SXTs. If that is the case, braking such as inverse Compton scattering must become important at temperatures lower than proposed in Supper & Trümper 2000, of  $kT \lesssim 30$  eV.

### 5.3. Ongoing low-level accretion

The interaction between a trickle of continuously accreting matter and the pulsar magnetosphere could potentially inhibit radio emission. There is precedent for variable low-level accretion in e.g. Cen X-4 (Cackett et al. 2010) and XTE J1701-462 (Fridriksson et al. 2011). A mechanism linking that accretion to the cessation of coherent radio emission was qualitatively described in Archibald et al. (2015) to explain the X-ray bright mode in J1023+0038. One may wonder whether some low-level accretion in the X-ray dim state of 1H 1905+000 remains, unnoticeable under the strict limits of  $\dot{M} \lesssim 10^{-13} M_{\odot} \text{ yr}^{-1}$  (Jonker et al. 2006). Yet even within that limit the rate would have to be sufficient to overcome the magneto-rotational plasma, the pulsar wind, to enter the pulsar light cylinder; bringing the system into the “propeller” accretion regime (Illarionov & Sunyaev 1975). Overall we find little evidence for this explanation for the dim state of 1H 1905+000.

### 5.4. Eclipses

The companion mass and orbital period of 1H 1905+000 are similar to those found in the “black-widow” (BW) MSP class (Roberts 2013). Those pulsars and the tMSPs are frequently eclipsed in radio as radio pulses are scattered by

the dense wind blown off the companion due to its evaporation (Luo & Melrose 1995). This is a possible explanation for our non-detection. Even though all three known tMSPs are redbacks, similar transitions might occur in BWs. However, short exposures and relatively little photon counts from Chandra X-ray observations of nearby BW MSPs (Gentile et al. 2014) make it difficult to prove a BW-tMSP scenario for 1H 1905+000 given its X-ray upper limits.

### 5.5. Lingering magnetic field burial

The formation of radio-pulsar emission requires a certain magnetic field strength. Yet accretion is thought to bury and diminish radio-pulsar magnetic fields during the transition from dead, normal pulsar to reborn tMSPs. Potentially, the magnetic field strength in 1H 1905+000 is now, after a prolonged period of accretion, too low to power the acceleration of primary charged particles.

Accretion rates above  $\dot{M} \simeq 0.03 \dot{m}_{\text{Edd}}$ , where  $\dot{m}_{\text{Edd}}$  is the Eddington accretion rate, are required for diamagnetic screening (“burial”) to be efficient (Cumming et al. 2001). The active-state mass accretion rate estimated to be required for 11 years of outbursts,  $\dot{M} \simeq 10^{-9} M_{\odot} \text{ yr}^{-1} \simeq 0.1 \dot{m}_{\text{Edd}}$  (Jonker et al. 2006) is larger and could thus bring about such screening. In that accretion steady state, the magnetic field was likely diminished by  $n \simeq (\dot{M}/0.02 \dot{m}_{\text{Edd}}) = 5$  orders of magnitude (Cumming 2008). In the most extreme outburst modelled in Cumming (2008), of 2 yr at  $0.05 \dot{m}_{\text{Edd}}$ , the magnetic field re-emerges on a  $\sim 1$  yr timescale (Fig. 2 in Cumming 2008 for a  $^{28}\text{Si}$  ocean). The significantly longer and more intense (11 yr,  $0.1 \dot{m}_{\text{Edd}}$ ) outburst of 1H 1905+000 may possibly be causing lingering magnetic field burial on the observed  $\sim 10$  yr timescale, preventing radio pulsations.

Given the quiescent mass transfer rate of  $10^{-13} M_{\odot} \text{ yr}^{-1}$  it might take around  $10^4$  yr to build up a new accretion disk of the same amount of mass (Jonker et al. 2006), and start a new active phase. Thus even in high-accretion rate systems such as 1H 1905+000 the magnetic field appears to have time to re-emerge, and effectuate radio-pulsar emission.

### 5.6. A low-magnetic field neutron star

Finally, as the accretion onto a NS lowers its magnetic field, large amounts of accreted matter may at some point demolish the electrical currents that supply NS magnetisation (Shibazaki et al. 1989; Romani 1990; Jahan Miri & Bhattacharya 1994). This can ultimately lead to a very large Ohmic magnetic field decay, resulting in a NS with an extremely low magnetic field (see, e.g., Tauris & Konar 2001). In regular pulsars such a long-term effect (Sang & Channugam 1987), reducing the magnetic field by four orders of magnitude, is well-known (and illustrated in Fig. 5). But as MSPs, like normal pulsars, can only shine above some “death line” (Chen & Ruderman 1993; Zhang et al. 2000), there is strong selection effect toward MSPs with magnetic field of at least  $10^8$  G. If 1H 1905+000 due to its accretion history now supports only an extremely low-strength down to  $B \simeq 10^7$  G (Zhang 2013) field, it would remain radio quiet. In this case, the NS would likely have had to accrete many tenths of solar masses overall, without collapsing to a black hole, as a significant number of MSPs that have gained similar weight in the past are still shining today (Antoniadis et al. 2016). If this is the reason 1H 1905+000 is not shining, it should be positioned in a region of the standard  $P - \dot{P}$  diagram (see Fig. 5) that is above its limiting magnetic field line, but below death



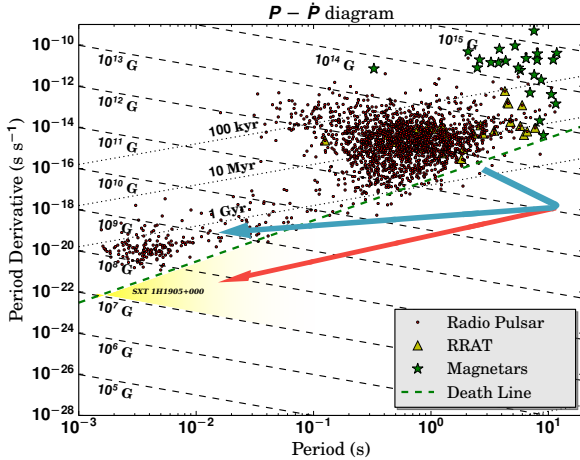


**Figure 5.** Two evolutionary scenarios for radio millisecond pulsars on a general  $P-\dot{P}$  diagram: a standard “recycling” evolution (Bhattacharya & van den Heuvel 1991, blue line) and a low magnetic field “reconfiguration” evolution (red line). Only the area segment between the limiting  $B \approx 10^7$  G line and the closest to known MSPs death line (green dashed line, see Fig. 1 from Zhang et al. 2000, line III’) is suitable for SXT 1H 1905+000. The brightness of the yellow area represents the positional probability of the transient.

line (e.g., Zhang et al. 2000), closest to the actual MSP population but as yet invisible.

## 6. CONCLUSION AND FUTURE WORK

Our Arecibo observations toward the dimmest known soft X-ray transient, 1H 1905+000, did not reveal pulsar emission in over a decade. We have set a strong limit on its pseudo luminosity at largest distance  $L_{\text{pseudo}}(d=10 \text{ kpc}) = 1.0 \text{ mJy kpc}^2$ . We are 85% confident that SXT 1H 1905+000 is presently not in the radio pulsar state. Future, more sensitive and simultaneous radio and X-ray observations might reveal the exact nature of SXTs and put more constraints on their potentially tight connection with the traditional MSP class. Additional gamma-ray observations could potentially shed light on the radio-beaming fraction and the radio-eclipse scenarios, and thus support more firmly our current conclusion: 1H 1905+000 is inherently radio quiet.

## ACKNOWLEDGEMENTS

We thank L. Bildsten, S. Ransom, G. Nelemans and I. Stairs for the discussions that started this project, and A. Archibald, R. Wijnands, and the referee for subsequent suggestions. The Arecibo Observatory is operated by SRI International under a cooperative agreement with the National Science Foundation (AST-1100968), and in alliance with Ana G. Méndez-Universidad Metropolitana, and the Universities Space Research Association. The research leading to these results has received funding from the European Research Council under the European Union’s Seventh Framework Programme (FP/2007-2013) / ERC Grant Agreement n. 617199, and from the Netherlands Research School for Astronomy (NOVA4-ARTS). We also thank SURF Cooperative and e-Science support center for provision and maintenance of the Dutch national supercomputer Cartesius and related resources. Computing time was provided by NWO Physical Sciences.

## REFERENCES

- Antoniadis, J., Tauris, T. M., Ozel, F., et al. 2016, ArXiv e-prints, [arXiv:1605.01665 \[astro-ph.HE\]](https://arxiv.org/abs/1605.01665)
- Archibald, A. M., Stairs, I. H., Ransom, S. M., et al. 2009, *Science*, **324**, 1411
- Archibald, A. M., Bogdanov, S., Patruno, A., et al. 2015, *ApJ*, **807**, 62
- Bassa, C. G., Patruno, A., Hessels, J. W. T., et al. 2014, *MNRAS*, **441**, 1825
- Bhattacharya, D. 1998, in NATO Advanced Science Institutes (ASI) Series C, Vol. 515, NATO Advanced Science Institutes (ASI) Series C, ed. R. Bucccheri, J. van Paradijs, & A. Alpar, 103
- Bhattacharya, D., & van den Heuvel, E. P. J. 1991, *Phys. Rep.*, **203**, 1
- Bilous, A. V., Pennucci, T. T., Demorest, P., & Ransom, S. M. 2015, *ApJ*, **803**, 83
- Bogdanov, S., & Halpern, J. P. 2015, *ApJ*, **803**, L27
- Brown, E. F., Bildsten, L., & Rutledge, R. E. 1998, *ApJ*, **504**, L95
- Burderi, L., & Di Salvo, T. 2013, *Mem. Soc. Astron. Italiana*, **84**, 117
- Burgay, M., Burderi, L., Possenti, A., et al. 2003, *ApJ*, **589**, 902
- Cackett, E. M., Brown, E. F., Miller, J. M., & Wijnands, R. 2010, *The Astrophysical Journal*, **720**, 1325
- Camilo, F., Lorimer, D. R., Freire, P., Lyne, A. G., & Manchester, R. N. 2000, *ApJ*, **535**, 975
- Campana, S., Colpi, M., Mereghetti, S., Stella, L., & Tavani, M. 1998, *A&A Rev.*, **8**, 279
- Chakrabarty, D., & Morgan, E. H. 1998, *Nature*, **394**, 346
- Chen, K., & Ruderman, M. 1993, *ApJ*, **402**, 264
- Coenen, T., van Leeuwen, J., & Stairs, I. H. 2011, *A&A*, **531**, A125
- Cordes, J. M. 2004, in Astronomical Society of the Pacific Conference Series, Vol. 317, Milky Way Surveys: The Structure and Evolution of our Galaxy, ed. D. Clemens, R. Shah, & T. Brainerd, 211
- Cordes, J. M., & Lazio, T. J. W. 2002, ArXiv Astrophysics e-prints, [astro-ph/0207156](https://arxiv.org/abs/astro-ph/0207156)
- Cumming, A. 2008, in American Institute of Physics Conference Series, Vol. 1068, American Institute of Physics Conference Series, ed. R. Wijnands, D. Altamirano, P. Soleri, N. Degenaar, N. Rea, P. Casella, A. Patruno, & M. Linares, 152
- Cumming, A., Zweibel, E., & Bildsten, L. 2001, *ApJ*, **557**, 958
- de Martino, D., Falanga, M., Bonnet-Bidaud, J.-M., et al. 2010, *A&A*, **515**, A25
- Deller, A. T., Mordon, J., Miller-Jones, J. C. A., et al. 2015, *ApJ*, **809**, 13
- Di Salvo, T., & Burderi, L. 2003, *A&A*, **397**, 723
- Dowd, A., Sisk, W., & Hagen, J. 2000, in Astronomical Society of the Pacific Conference Series, Vol. 202, IAU Colloq. 177: Pulsar Astronomy - 2000 and Beyond, ed. M. Kramer, N. Wex, & R. Wielebinski, 275
- Fridriksson, J. K., Homan, J., Wijnands, R., et al. 2011, *ApJ*, **736**, 162
- Galloway, D. K., Muno, M. P., Hartman, J. M., Psaltis, D., & Chakrabarty, D. 2008, *ApJS*, **179**, 360
- Gentile, P. A., Roberts, M. S. E., McLaughlin, M. A., et al. 2014, *ApJ*, **783**, 69
- Haensel, P., & Zdunik, J. L. 2003, *A&A*, **404**, L33
- Hartman, J. M., Patruno, A., Chakrabarty, D., et al. 2009, *ApJ*, **702**, 1673
- . 2008, *ApJ*, **675**, 1468
- Haslam, C. G. T., Salter, C. J., Stoffel, H., & Wilson, W. E. 1982, *A&AS*, **47**, 1
- Iacolina, M. N., Burgay, M., Burderi, L., Possenti, A., & di Salvo, T. 2010, *A&A*, **519**, A13
- Illarionov, A. F., & Sunyaev, R. A. 1975, *A&A*, **39**, 185
- Jahan Miri, M., & Bhattacharya, D. 1994, *MNRAS*, **269**, 455
- Jaodand, A., Archibald, A. M., Hessels, J. W. T., et al. 2016, *ApJ*, **830**, 122
- Johnston, T. J., Ray, P. S., Roy, J., et al. 2015, *ApJ*, **806**, 91
- Johnston, H. M., & Kulkarni, S. R. 1991, *ApJ*, **368**, 504
- Jonker, P. G., Bassa, C. G., Nelemans, G., et al. 2006, *MNRAS*, **368**, 1803
- Jonker, P. G., & Nelemans, G. 2004, *MNRAS*, **354**, 355
- Jonker, P. G., Steeghs, D., Chakrabarty, D., & Juett, A. M. 2007, *ApJ*, **665**, L147
- Kardashëv, N. S., Mitrofanov, I. G., & Novikov, I. D. 1984, *Soviet Ast.*, **28**, 651
- Knight, H. S. 2006, *Chinese Journal of Astronomy and Astrophysics Supplement*, **6**, 41
- Lawson, K. D., Mayer, C. J., Osborne, J. L., & Parkinson, M. L. 1987, *MNRAS*, **225**, 307
- Linares, M., Bahramian, A., Heinke, C., et al. 2014, *MNRAS*, **438**, 251
- Lorimer, D. R. 2008, *Living Reviews in Relativity*, **11**, 8
- Luo, Q., & Melrose, D. B. 1995, *ApJ*, **452**, 346
- Manchester, R. N., Hobbs, G. B., Teoh, A., & Hobbs, M. 2005, *AJ*, **129**, 1993
- Maron, O., Kijak, J., Kramer, M., & Wielebinski, R. 2000, *A&AS*, **147**, 195
- McLaughlin, M. A., Lyne, A. G., Lorimer, D. R., et al. 2006, *Nature*, **439**, 817
- Mikhailov, K., & van Leeuwen, J. 2016, *A&A*, **593**, A21
- Papitto, A., de Martino, D., Belloni, T. M., et al. 2015, *MNRAS*, **449**, L26



- Papitto, A., Hessels, J. W. T., Burgay, M., et al. 2013, The Astronomer's Telegram, 5069, 1
- Patruno, A., & Watts, A. L. 2012, ArXiv e-prints, [arXiv:1206.2727 \[astro-ph.HE\]](#)
- Patruno, A., Jaodand, A., Kuiper, L., et al. 2016, ArXiv e-prints, [arXiv:1611.06023 \[astro-ph.HE\]](#)
- Ransom, S. M. 2001, PhD thesis, Harvard University
- Ransom, S. M., Cordes, J. M., & Eikenberry, S. S. 2003, *ApJ*, **589**, 911
- Roberts, M. S. E. 2013, in *IAU Symposium, Vol. 291, IAU Symposium*, ed. J. van Leeuwen, 127
- Romani, R. W. 1990, *Nature*, **347**, 741
- Roy, J., Ray, P. S., Bhattacharyya, B., et al. 2015, *ApJ*, **800**, L12
- Sang, Y., & Chanmugam, G. 1987, *ApJ*, **323**, L61
- Shibazaki, N., Murakami, T., Shaham, J., & Nomoto, K. 1989, *Nature*, **342**, 656
- Stappers, B. W., Archibald, A., Bassa, C., et al. 2013, The Astronomer's Telegram, 5513
- Stappers, B. W., Archibald, A. M., Hessels, J. W. T., et al. 2014, *ApJ*, **790**, 39
- Stella, L., Campana, S., Colpi, M., Mereghetti, S., & Tavani, M. 1994, *ApJ*, **423**, L47
- Strader, J., Chomiuk, L., Cheung, C. C., et al. 2015, *ApJ*, **804**, L12
- Sun, X.-H., & Reich, W. 2010, *Research in Astronomy and Astrophysics*, **10**, 1287
- Supper, R., & Trümper, J. 2000, *A&A*, **357**, 301
- Takata, J., Li, K. L., Leung, G. C. K., et al. 2014, *ApJ*, **785**, 131
- Tam, P. H. T., Li, K. L., Kong, A. K. H., et al. 2014, ArXiv e-prints, [arXiv:1412.4985 \[astro-ph.HE\]](#)
- Tauris, T. M., & Konar, S. 2001, *A&A*, **376**, 543
- van Leeuwen, J., Kasian, L., Stairs, I. H., et al. 2015, *ApJ*, **798**, 118
- Wijnands, R., & van der Klis, M. 1998, *Nature*, **394**, 344
- Yakovlev, D. G., Gasques, L., & Wiescher, M. 2006, *MNRAS*, **371**, 1322
- Yakovlev, D. G., & Pethick, C. J. 2004, *ARA&A*, **42**, 169
- Yusifov, I., & Küçük, I. 2004, *A&A*, **422**, 545
- Zhang, B., Harding, A. K., & Muslimov, A. G. 2000, *ApJ*, **531**, L135
- Zhang, B., Qiao, G. J., Lin, W. P., & Han, J. L. 1997, *ApJ*, **478**, 313
- Zhang, C. M. 2013, in *IAU Symposium, Vol. 291, Neutron Stars and Pulsars: Challenges and Opportunities after 80 years*, ed. J. van Leeuwen, 583